



# Coot Algorithm for Optimal Carbon–Energy Combined Flow of Power Grid With Aluminum Plants

Liangdong Qin<sup>1</sup>, Tianfeng Xu<sup>1</sup>, Sheng Li<sup>2\*</sup>, Zhiyong Chen<sup>1</sup>, Qianmao Zhang<sup>1</sup>, Jiahui Tian<sup>1</sup> and Yujun Lin<sup>2</sup>

<sup>1</sup>State Grid Hebei Electric Power Co., Ltd., Shijiazhuang, China, <sup>2</sup>State Key Laboratory of Advanced Electromagnetic Engineering and Technology, School of Electrical and Electronic Engineering, Huazhong University of Science and Technology, Wuhan, China

To achieve a low-carbon and economical operation for the power grid, this paper proposes a novel optimal carbon–energy combined flow (OCECF) by considering the influence of aluminum plants. It attempts to minimize the carbon emission of power grid, power loss, and the voltage deviation by taking the reactive power control of aluminum plants into account. Since the presented OCECF is a nonlinear and complex optimization problem, a new metaheuristic algorithm called Coot algorithm is employed to acquire a high-quality dispatch solution under various scenarios. The Coot algorithm is inspired by the movement of birds on the water surface, which can implement a wide exploration via the random movement and a deep exploitation via the chain movement with the group leaders. The performance of Coot algorithm for the presented OCECF is carried out on an IEEE 57-bus system with various power plants, in which the group search optimizer is introduced for performance comparison.

**Keywords:** carbon–energy combined flow, coot algorithm, aluminum plants, power grid, meta-heuristic algorithm

## OPEN ACCESS

### Edited by:

Yaxing Ren,  
University of Warwick,  
United Kingdom

### Reviewed by:

Lefeng Cheng,  
Guangzhou University, China  
Linfei Yin,  
Guangxi University, China  
Chuangzhi Li,  
Shantou University, China

### \*Correspondence:

Sheng Li  
sgord2@163.com

### Specialty section:

This article was submitted to  
Smart Grids,  
a section of the journal  
Frontiers in Energy Research

**Received:** 17 January 2022

**Accepted:** 27 January 2022

**Published:** 09 June 2022

### Citation:

Qin L, Xu T, Li S, Chen Z, Zhang Q,  
Tian J and Lin Y (2022) Coot Algorithm  
for Optimal Carbon–Energy Combined  
Flow of Power Grid With  
Aluminum Plants.  
Front. Energy Res. 10:856314.  
doi: 10.3389/ferng.2022.856314

## 1 INTRODUCTION

In recent years, atypical weather patterns have resulted in the frequency of natural disasters, such as earthquake, flooding, and forest fires in the world, which directly related to the increasing production of carbon dioxide (CO<sub>2</sub>) (Walther et al., 2002). The global temperature is increasing year by year due to the increase in the content of greenhouse gases in the atmosphere, and these are mainly caused by human activities. Among them, carbon dioxide is the most distinctive greenhouse gas. It shows that with the rapid development of the industry, environmental problems are becoming more and more severe and pose a threat to human health at the same time. The advocacy of low carbon life becomes inevitable, and the reduction in CO<sub>2</sub> has attracted extensive attention in both industry and research. In such a low-carbon–energy transition era, electric power industry, as a prime CO<sub>2</sub> producer, takes on greater responsibility for reducing carbon emissions from the generation side of electricity and from transmission flows. A lot of investigations have been concentrated on low-carbon electric power. From the point of view of environmental economy, clean energy technologies, such as carbon capture and storage technologies are key to reducing emissions in the current scenario where the power sector relies on emission-intensive energy resources (Wei et al., 2016). In Ghorbani (2016), Song et al. proposed nonconvex planning for economic scheduling of CHP in various integrated cogeneration systems using exchange market algorithms. Power grid companies have been trying to find more reasonable resource dispatching solutions to rationally allocate power resources according to customer demand and optimize the distribution system to achieve the most economical and

quality system operation (Carpentier et al., 1996). Liu et al. (2014) proposed a multistage scenario tree-based approach, which uses a rolling scheduling scheme to consider the uncertainty of solar energy, nondispatchable power, and thermal loads in the operation of building energy systems using uncertainty information updated every hour.

Due to the difference in emission levels, carbon emissions are bound to the scheduling process by imposing penalties on carbon generation. However, the existing penalty methods are still inadequate. A penalty-based approach to resource scheduling, minimizing the cost of carbon emissions penalties/environmental loss, is proposed in Liu et al. (2014) to allocate switching states and power distribution. Existing studies aim to reduce the generation of total carbon emissions and ignore the carbon emissions of the electricity network, which is closely related to the interests of the grid companies. To effectively deal with this challenge, an optimal carbon–energy combined flow (OCECF) for electricity networks was suggested in Kang et al. (2012), Li et al. (2013), Zhang et al. (2015), and Zhang et al. (2018), where the tracking method identifies carbon liability with full electricity consumer responsibility. The literature (Lassagne et al., 2013) shows that in industrial processes, such as aluminum production, it has been observed that the CO<sub>2</sub> levels in the fume capture the economic variability of the equipment. Moreover, due to the inherent characteristics of the wastewater generated by virgin aluminum refinery, the present methods of carbon trapping technology cannot be used directly. Therefore, studies have shown that it cannot be applied to the measurement of CO<sub>2</sub> emissions from power networks, including aluminum plants. Aluminum plants have some typical characteristics, such as heavy load and reactive voltage regulation demand, which should be factored into the OCECF. OCECF is a model characterized by nonlinear programming with multivariate and complex constraints. It usually has two techniques, namely, traditional optimization methods, heuristic algorithms, and metaheuristic algorithms. Traditional optimization algorithms like mixed-integer linear programming (Gan et al., 2019), De Casteljau's algorithm (Zhou et al., 2021a), and reduced event-base algorithm (Zhou et al., 2021b) rely mainly on the precise magnetic pattern of a particular optimum, and it can easily fall into a local optimum for nonlinear multipole planning with noncontinuous features and restraints. In comparison, the metaheuristic algorithm Coot algorithm can have better performance than the heuristic algorithm, such as faster convergence and more accurate characteristics. A new krill swarm was proposed in Adhvaryu et al. (2017), which was successfully applied to dynamic optimum energy tracking for combined heating and power systems. In Abbas et al. (2017), G. Abbas et al. discuss in detail various hybrid forms of particle swarm algorithms and perform in-depth nonconvex economic scheduling based on particle swarm optimization. Genetic algorithms are applied to microgrids, and a genetic algorithm-based optimizer is designed for the economic dispatch of microgrids with renewable energy sources. The metaheuristic algorithm is a stochastic algorithm for finding the best response.

A classification of optimality methods and approximation algorithms is made into two categories: precise and proximate algorithms. Precise algorithms are able to find the best answer accurately. However, they are inefficient sufficiently for demanding optimality issues, and their implementation duration grows exponentially with the dimension of the problem. Proximate algorithms are able to identify close to optimal solutions for rigorous optimization problems in a relatively short period of time. The development of metaheuristic algorithms was motivated by biological processes, the behavior of animals, and the concept of conservation and human activity. Based on the collective behavior of birds, a new optimization algorithm, Coot, simulates the movement of cores on water with a metaheuristic algorithm applied to the OCECF model in this paper, which has a better performance for power grid containing aluminum plants.

The next section of this article is structured as described below: The *Numerical simulation of optimal carbon–energy combined flow* **Section 2** describes the numerical simulation of the OCECF with the participation of the aluminum plants. The *Coot optimization algorithms for optimal carbon–energy combined flow* **Section 3** describes the basic principles of the Coot algorithm. The *Design of Coot for optimal carbon–energy combined flow* **Section 3.3** develops the design of the Coot algorithm for OCECF, and the *Case studies* **Section 4** presents the simulation results of the Coot algorithm for the constructed problem. Last, the *Conclusion* **Section 5** draws the conclusion of this article.

## 2 NUMERICAL SIMULATION OF OPTIMAL CARBON–ENERGY COMBINED FLOW

### 2.1 Carbon–energy combined flow

In the existing studies, the carbon emission statistics are usually obtained by converting primary energy consumption to macroscopic statistics. These methods cannot reveal the characteristics of carbon emissions in power systems, and there are many limitations in their application. The concept of power system carbon emission flow in **Figure 1** is proposed to combine carbon emission analysis with power system tide calculation, which provides new ideas for the research in the field of low carbon power. A power system carbon stream is defined as a virtual network stream that is dependent on the power tide and is used to characterize the carbon characteristics of electric power systems that maintain the tide in either path (Kang et al., 2012). For carbon flows, not only do factors such as grid topology, generator output power, and nodal power demand fluctuate, but they are notably driven by the carbon intensity of the generators and the shared liability between the power producers and the users of the energy. The calculation of CO<sub>2</sub> flow is based mainly on the obtained tide of the power system, where the carbon emissions of the entire electrical system are equivalent to the CO<sub>2</sub> emissions of the generation side  $C_p$ . Therefore, it can be described as the accumulation of the grid losses  $C_{loss}$  and demand-side carbon emissions  $C_d$ , as described below:

$$C_p = \sum_{w \in W} P_w \delta_w = C_d + C_{loss} \quad (1)$$

where  $P_w$  in the formula represents the delivery power of the  $w$ th generator,  $\delta_w$  means the carbon emission intensity of the  $w$ th generator, and  $W$  is the total generator set.

Theoretically, electricity producers, i.e., power generators as well as grid companies, are primarily concerned with their own carbon emission quantities and footprints (Liu et al., 2014). For electricity users and consumers, they are concerned with the amount of their own carbon emissions. Therefore, analyzing only the first two will inevitably lead to multiple calculations of carbon emissions, lacking consideration of the co-responsibility component. To better refine this issue, the shared responsibility algorithm appropriately decomposes the overall carbon emissions of electricity producers and consumers as described below:

$$C_p = (1 - \alpha_p)C_e + \alpha_p C_{loss} + (1 - \beta_c)\alpha_p C_L + \alpha_p \beta_c C_L \quad (2)$$

where  $\alpha P$  is the share of the producer responsibility, and the value of  $\alpha P$  is between 0 and 1. This means that it is not the party producing the electricity that is responsible for all the carbon emissions; only the  $\alpha P$  portion is accounted for, and  $\beta C$  represents the share of the consumer responsibility,  $0 < \beta C < 1$ . Similarly, the party that uses the electricity load is not only responsible for its own carbon emissions from electricity use but also shares a portion  $\beta C$  of the carbon emissions used for electricity production.

As the grid company, the first priority is to focus on energy and flow through tidal analysis, as well as functional energy power losses along with an obligation for carbon emissions associated with carbon flows. The power losses can be described as described below:

$$P_{loss} = \sum_{i,j \in N_L} g_{ij} [V_i^2 + V_j^2 - 2V_i V_j \cos \theta_{ij}] \quad (3)$$

where  $V_i$  and  $V_j$  denote the size between the voltage of the  $i$ th and  $j$ th nodes, and  $g_{ij}$  represents the electrical conductivity of line  $i - j$ ;  $\theta_{ij}$  means the variation of voltage phasor angle (node  $i$  and  $j$ ), and  $N_L$  shows the branch set.

Therefore, the power network companies also have a corresponding carbon emission duty  $C_{pgc}$ , which could be calculated according to (2):

$$C_{pgc} = \alpha_p C_{loss} + (1 - \beta_c)\alpha_p C_L \quad (4)$$

where  $C_{loss}$  needs to be calculated based on the proportionate allocation rule to obtain, and the proportional sharing principle can be shown as follows:

$$C_{ds} = \sum_{i,j \in N_L} \sum_{w \in W} \left( \frac{\alpha_{jw}^{(-1)} \Delta P_{ij}}{P_j'} \right) P_w \delta_w \quad (5)$$

where  $\alpha_{jw}^{(-1)}$  is convenient to depict the power coefficient of energy maps between the  $j$ th node and  $w$ th generator,  $P_{ij}$  and  $P_j'$  indicate the functional energy power losses of line  $i - j$  and the gross power flow of the  $j$ th node in the equivalent lossless grid separately.

## 2.2 Optimal carbon–energy combined flow model

There are several factors affecting the combined flow of carbon–energy, the strongest of which are functional energy power dispatch and redundant power scheduling (Zhang et al., 2015). Among them, functional energy power dispatch is decided by electricity generators, network utilities, and power clients; redundant power scheduling is mainly manipulated by power network companies. Hence, the OCECF model is described by the reactive power dispatch after the functional energy power dispatch, while minimizing their own carbon liabilities, functional energy power losses, and voltage deviations, where the aim feature could be expressed by a nonlinear weighting approach, as shown below:

$$\min f(x) = \mu_1 P_{loss} + \mu_2 C_{pgc} + \mu_3 V_d \quad (6)$$

subject to

$$\left\{ \begin{array}{l} P_{Gi} - P_{Di} - V_i \sum_{j \in N_i} V_j (g_{ij} \cos \theta_{ij} + b_{ij} \sin \theta_{ij}) = 0 \\ Q_{Gi} - Q_{Di} - V_i \sum_{j \in N_i} V_j (g_{ij} \sin \theta_{ij} - b_{ij} \cos \theta_{ij}) = 0 \\ Q_{Gi}^{\min} \leq Q_{Gi} \leq Q_{Gi}^{\max}, i \in N_G \\ V_{Ci}^{\min} \leq V_i \leq V_{Ci}^{\max}, i \in N_i \\ Q_{Ci}^{\min} \leq Q_{Ci} \leq Q_{Ci}^{\max}, i \in N_C \\ T_k^{\min} \leq T_k \leq T_k^{\max}, k \in N_T \\ |S_l| \leq S_l^{\max}, l \in N_L \end{array} \right. \quad (7)$$

where  $x$  means the vector of the subsystem, which can substitute the voltage of the generator terminals, individual tapping location of the on-load tap-changer (OLTC) transformer, total number of capacitors and inductors connected, etc.;  $V_d$  means the voltage deviation index;  $\mu_1, \mu_2$ , and  $\mu_3$  are corresponding weight factor to various targets, respectively, and each variable takes a value between 0 and 1, and the sum of the values of the three variables is 1.

The first two equations in Eq. (7) are the tidal balance codes, which can be used to constrain the active and reactive tidal balances as equations for the decentralized OCECF, in which  $P_{Gi}$  and  $Q_{Gi}$  are the functional energy power and redundant power delivery of the  $i$ th node. The third and fourth equations in Eq. (7) are derived from the generator constraint equation, which means that the redundant power delivery and the generating busbar voltage are subject to their upper and lower limits. The fifth equation is the shunt capacitor constraint, since the reactive power compensation of controlled shunt capacitors can only run within their minimum and maximum limits, so,  $Q_{Ci}$  describes the redundant power compensation of the  $i$ th node. Due to the tap position of the transformers being restricted by their minimum and maximum limits, so with the sixth formula in Eq. (7),  $T_k$  is the transformer tap ratio. So as to acquire secure functioning of all subsystems, the size of the voltage of the burden bus is limited by its lower limit, and the apparent power flow of each transmission line is limited by its upper limit, so with the last equation constraint in Eq. (7), and  $S_l$  stands for the power apparent on transmission line  $l$ . In the formula above,  $N_i$  is the node group,  $N_G$  is the unit group,  $N_C$  means the group of

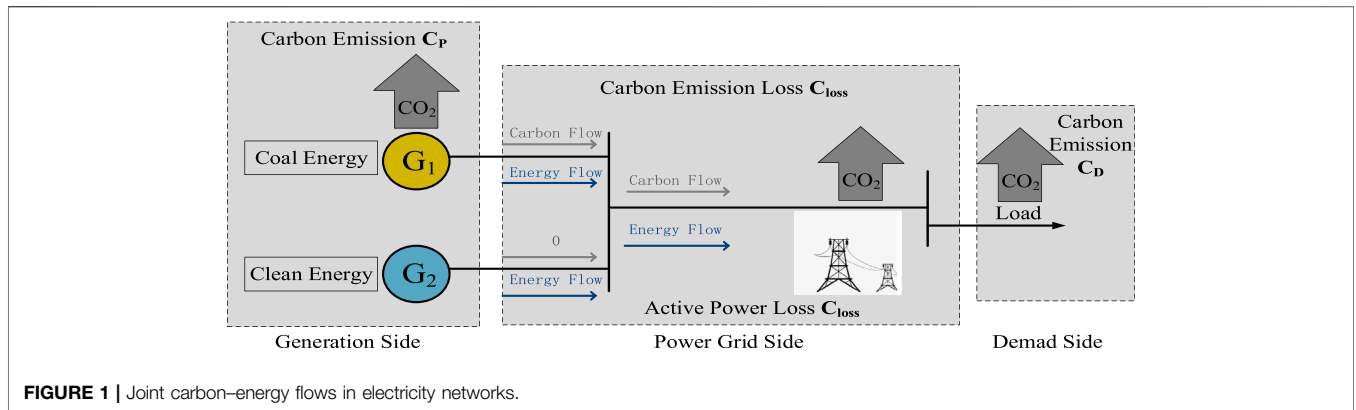


FIGURE 1 | Joint carbon–energy flows in electricity networks.

compensation facilities, *NT* means the tapped group of transformers, and *NL* means the group of the branches.

Besides, the deviation index of voltage can be described as below:

$$V_d = \sum_{i \in N_i} \left| \frac{2V_i - V_i^{max} - V_i^{min}}{V_i^{max} - V_i^{min}} \right| \quad (8)$$

### 2.3 Characteristics of aluminum plant load

As the second richest ingredient in the Earth’s capsule behind oxygen and silicon, aluminum is being used more and more widely in various fields with the rapid progress of modern chemical industry, agriculture, and science and technology (Cook et al., 2007). Since its special properties, aluminum has played a very crucial role in the flourishing of important industries, such as aviation, construction, and automobiles. So, it is essential to pay attention to the aluminum plant load.

The power supply system of an aluminum plant consists of four main components: transformer, motor, line, and load, and the load of an aluminum plant consists of two components: the power load as well as the electrolytic aluminum. The auxiliary facilities for aluminum electrolysis are mainly power loads. The power load is started before the aluminum electrolysis load is started, and the power load can only be stopped after the aluminum electrolysis load is withdrawn.

During normal operation, the aluminum electrolytic load cannot be quickly batched out in a short period of time. During the scheduled maintenance period of the electrolyzer, it is necessary to open and close the electrolyzer. In this case, it is inevitable to gradually reduce the current until the operation of short junctions begins and then to raise the current to normal values. In the planned maintenance of the electrolyzer, the time for opening and stopping it to operate its short-circuit position is not very long, but it is still necessary to ensure the continuity of a power plant-generating unit start-up as much as possible. There are some distinctive features of aluminum plant loads, such as large loads and high reactive voltage regulation requirements, so it is more important to take them into account in the OCECF model. Loads like the aluminum

plant absorb reactive power from the grid and reduce the power factor. The low power factor increases not only the power loss in the power supply and distribution system but also the voltage loss and reduces the utilization rate of the power supply equipment. From Eqs. (9) and (10), it can be seen that providing reactive power compensation and reducing reactive power is an effective action to improve the power factor. Therefore, reactive power compensation devices must be used in a targeted manner to improve the power factor for such loads. The vector diagram in Figure 2 clearly demonstrates the need to provide reactive power compensation and improve the power factor.

$$\cos\varphi = \frac{P}{S} = \frac{P}{\sqrt{P^2 + Q^2}} \quad (9)$$

$$\cos\varphi = \frac{P}{S} = \frac{P}{\sqrt{P^2 + (Q - Q^*)^2}} \quad (10)$$

## 3 COOT OPTIMIZATION ALGORITHMS FOR OPTIMAL CARBON-ENERGY COMBINED FLOW

### 3.1 Optimization principle

Coots are tiny fisher birds with numerous behaviors and maneuvers on the surface, as shown in Figure 3. As with the multiple leader PSO, it does not have a velocity argument. As a new evolutionary learning approach (Naruei and Keynia, 2021), the Coot algorithm has emerged from a study on them. The coots have diverse communal actions, and our aim in this document is to emulate group motion, i.e., both routine and nonroutine locomotion on the aquatic plane. The entire syndicate is guided toward the goal by the coot in front of the group and instructions from the coot ahead, which we define as the leader of the group. It has been found that coots have four separate motions on the aquatic surface, including random movement to this side and that side, chain movement, adjusting the position based on the group leaders, and leading the group by the leaders toward the optimal area (leader movement) (Memarzadeh and Keynia, 2021).

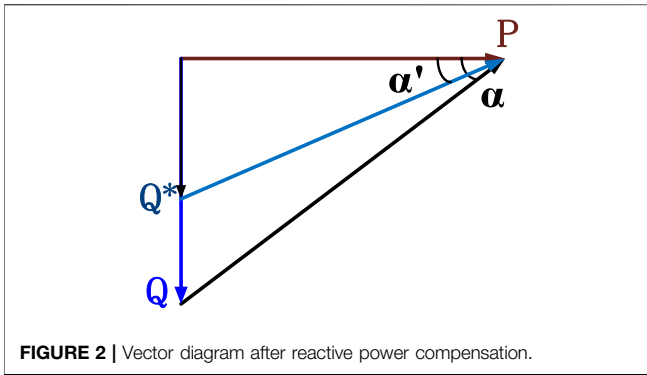


FIGURE 2 | Vector diagram after reactive power compensation.

TABLE 1 | The parameters used in Coot.

Parameter	Online optimization
$P$	0.5
$N_L$	5
$N_{COOT}$	45
$MaxIter$	50

The course of the procedure of the algorithm could be described in detail as below:

- 1) Initialization: A random population solution set is generated in the settlement field to form the primed population. The position of the  $i$ th Coot can be confirmed by  $Cootpos(i)$ , and  $d$  is the set of decision variables. The minimum and maximum bounds of the specification variations are scheduled for  $ub$  and  $lb$ , and the equation can be shown as follows:

$$Cootpos(i) = rand(1, d) * (ub - lb) + lb \quad (11)$$

After the initial overall is generated, the target problem is computed by comparing the objective function for each coot's

individual position. Meanwhile,  $N_L$  (number of leaders) and  $N_{COOT}$  (number of coots) are picked at random. The core of the algorithm is to look for the perfect coot or leader as holistically optimal at each step.

- 2) Position update: During the iterations, the coot's location on the water is updated according to the four movements already mentioned above.

### 3.2 Four types of movement for coots

- 1) Random movement to this side and that side: In this motion, first, considering a stochastic location in the field of search and shift the coot to this stochastic location, named  $Q$ , is generated using formula (9). Besides, since the coot movement exploring many different sections of the field of the search, to prevent the result from getting stuck in a locally optimal position, formula (12) is used to update the position of the coot.

$$Cootpos(i) = Cootpos(i) + A * R_2 * (Q - Cootpos(i)) \quad (12)$$

where  $R_2$  denotes a random number between 0 and 1, and  $A$  can be shown according to formula (13).

$$A = 1 - iter * \left( \frac{1}{MaxIter} \right) \quad (13)$$

in which  $iter$  is the current iteration, and  $MaxIter$  denotes the maximum iteration.

- 2) Chain movement: There are two types of chain motion: one uses the even orientation of the two coots to achieve group motion, and another way to achieve chain motion is to first figure out the range of distance vector from two movers and shift it to another mover with a distance vector of about half. We used the first method, and the formula can be shown as follows:

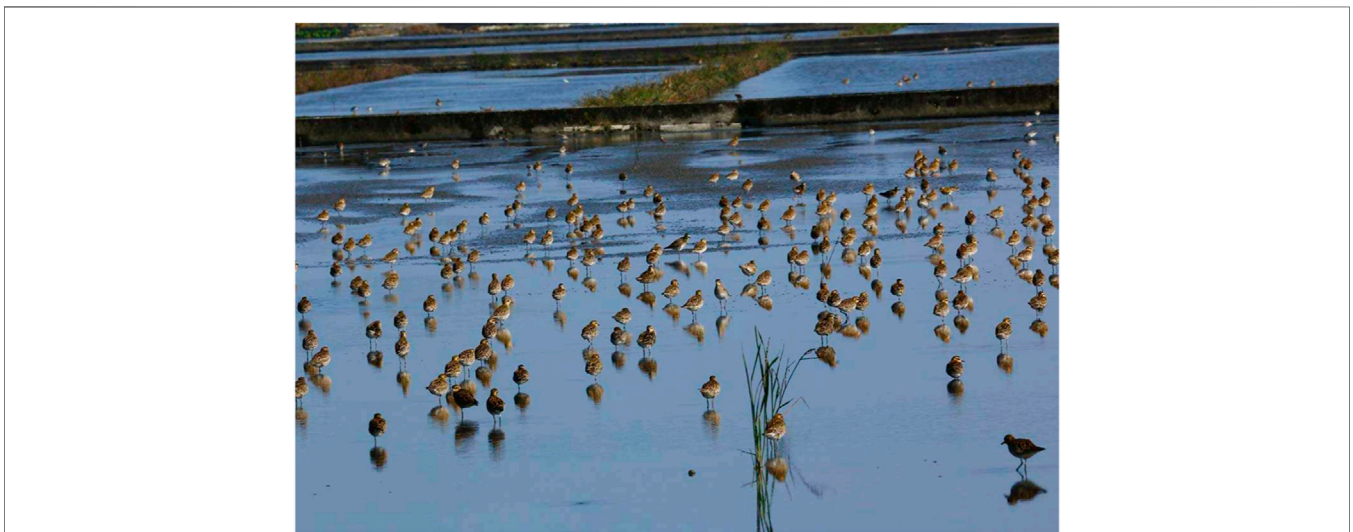
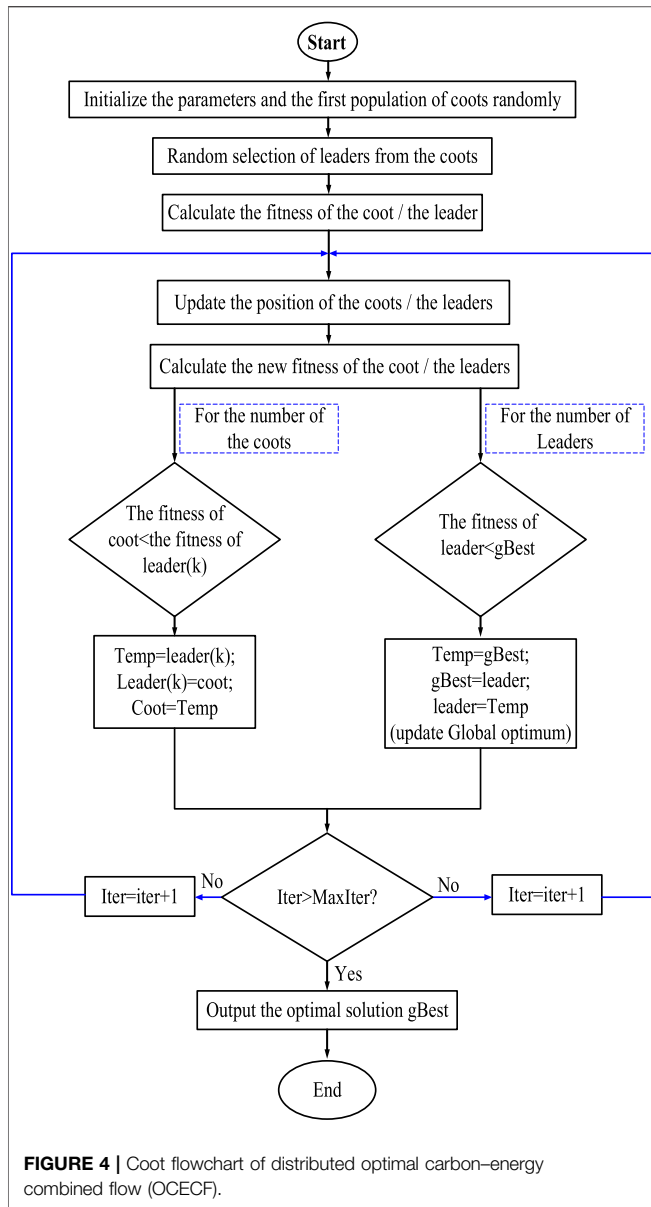


FIGURE 3 | A chain of coots moving on the surface of the water.



**FIGURE 4 |** Coot flowchart of distributed optimal carbon-energy combined flow (OCECF).

$$Cootpos(i) = 0.5 * (Cootpos(i - 1) + Cootpos(i)) \quad (14)$$

in which  $Cootpos(i - 1)$  denotes the position of the second coot.

3) Adjusting the position based on the group leaders: Normally, the group is led by some coots' group in front of it, and the rest of the coot must adjust their position according to the group leader and move closer to them, but a problem that may arise is that each coot adjusts its position according to the leader in the group. Therefore, it can be done by considering the average position of the leaders, and the coot updates its position according to this average position. Since considering the average position has the potential to lead to premature convergence, to achieve this movement, we use a mechanism to select leaders according to Eq. 15.

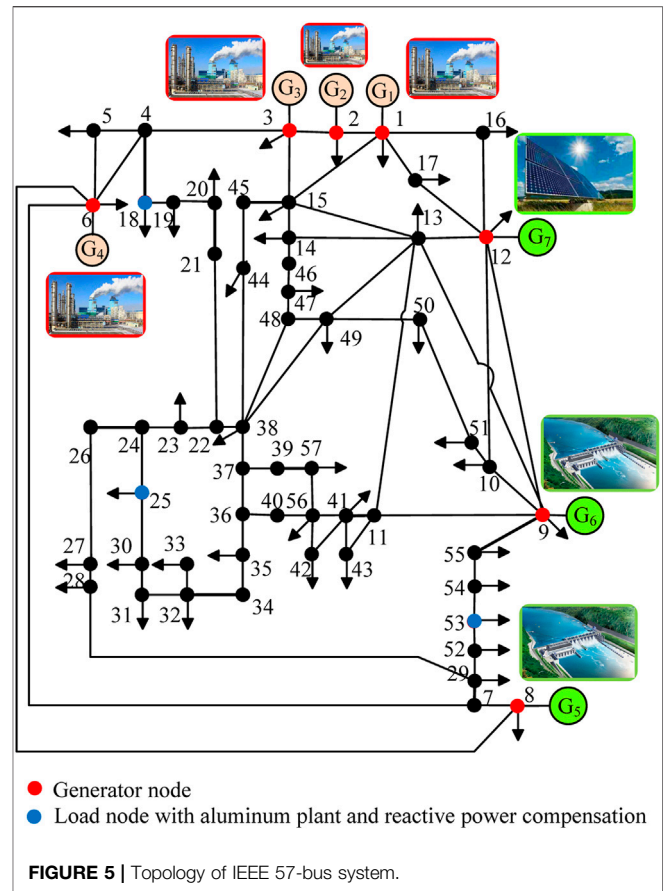


**FIGURE 5 |** Topology of IEEE 57-bus system.

**TABLE 2 |** CO<sub>2</sub> emission intensity of generators in IEEE 57-bus system.

Node of the generators	$\delta_w$ (kg/kWh)
1	1.01
2	0.95
3	1.5
6	0.7
8	0
9	0
12	0

$$K = 1 + (i \text{ MOD } N_L) \quad (15)$$

where  $i$  denotes the reference value of the current coot, and  $K$  denotes the reference value of the leaders.

$$Cootpos(i) = Leaderpos(k) + 2 * R1 * \text{COS}(2R\pi) * (LeadersPos(k) - Cootpos(i)) \quad (16)$$

In Eq. 16,  $Cootpos(i)$  shows the current position of coot;  $LeaderPos(k)$  denotes the selected leaders' position, R1 means a random number between 0 and 1, and R denotes a random number between -1 and 1.

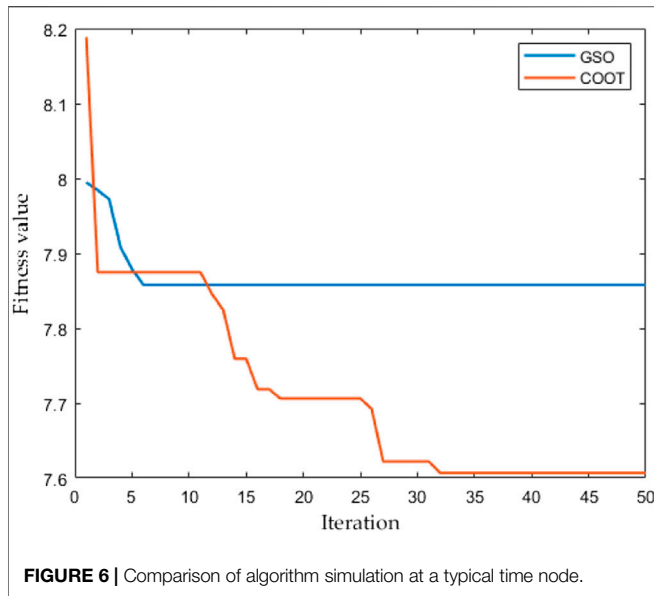


FIGURE 6 | Comparison of algorithm simulation at a typical time node.

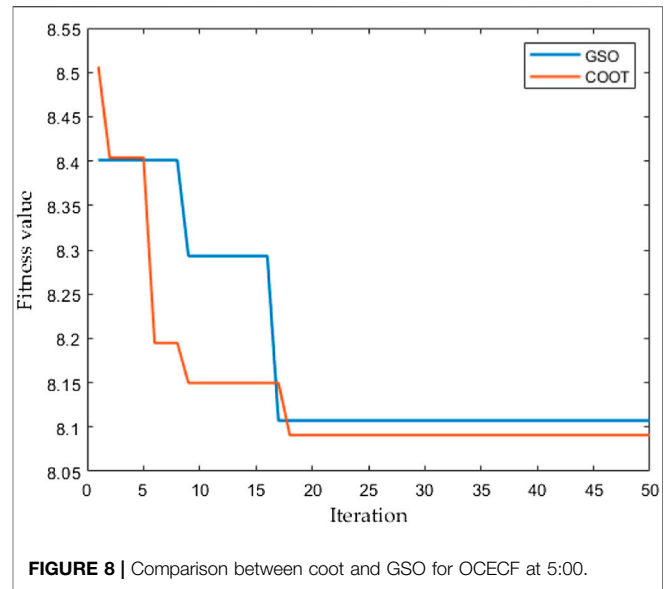


FIGURE 8 | Comparison between coot and GSO for OCECF at 5:00.

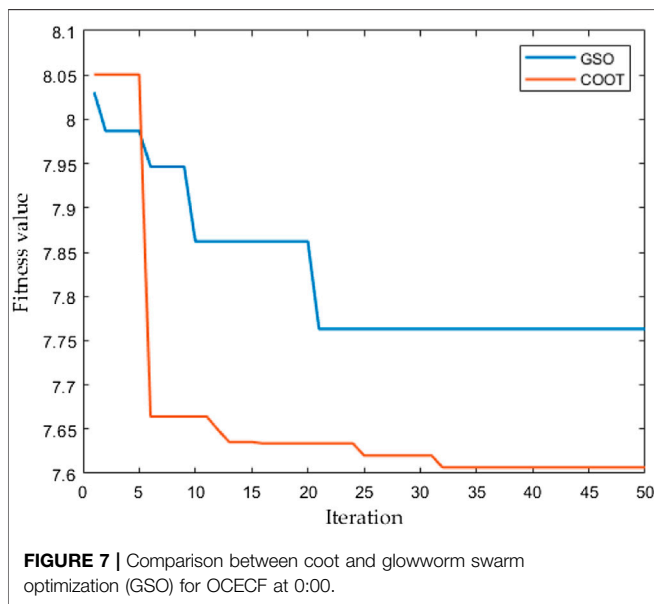


FIGURE 7 | Comparison between coot and glowworm swarm optimization (GSO) for OCECF at 0:00.

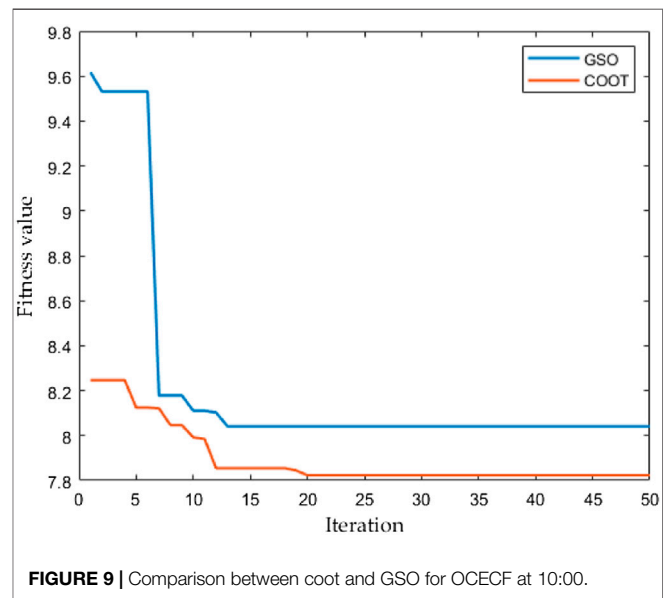


FIGURE 9 | Comparison between coot and GSO for OCECF at 10:00.

4) Leading the group by the leaders toward the optimal area (leader movement): To direct the team to the target area, the optimal area, the leader needs to continually update their position on the target during the iterative process. The leader's position can be better updated using Eq. (9). This formula is used to find a better position around the best position point of the current iteration around this current best point. There are some special cases where the leader must be made to move away from the current best position in order for the population to find a better position. Hence, the formula below provides a good way to approach the optimal position.

$$Leaderpos(i) = \begin{cases} B \cdot R3 \cdot \cos(2R\pi) \cdot (gBest - LeaderPos(i)) + gBest & R4 < 0.5 \\ B \cdot R3 \cdot \cos(2R\pi) \cdot (gBest - LeaderPos(i)) - gBest & R4 \geq 0.5 \end{cases} \quad (17)$$

where gBest signs the optimal location of the ever iteration, random numbers R3 and R4 take values between 0 and 1, random number R is in the interval [-1,1], and B should be found based on formula (18).

$$B = 2 - L \cdot \left( \frac{1}{maxiter} \right) \quad (18)$$

A larger random motion can be generated by B\*R3 in Eq. 17, preventing the algorithm from falling into a locally optimal

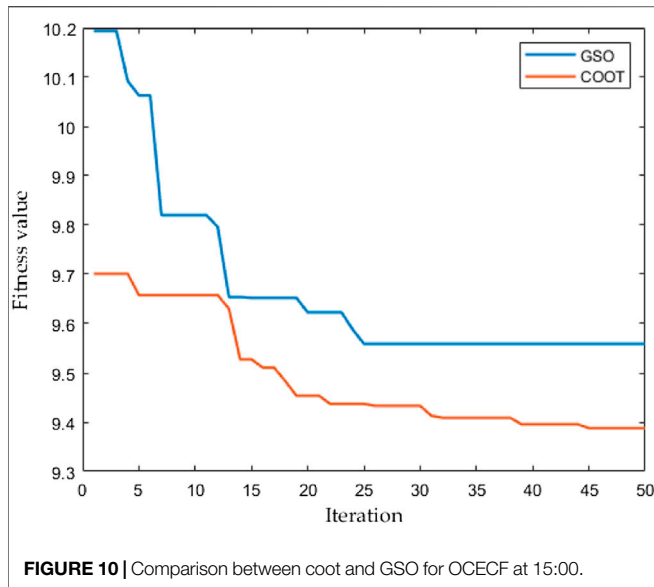


FIGURE 10 | Comparison between coot and GSO for OCECF at 15:00.

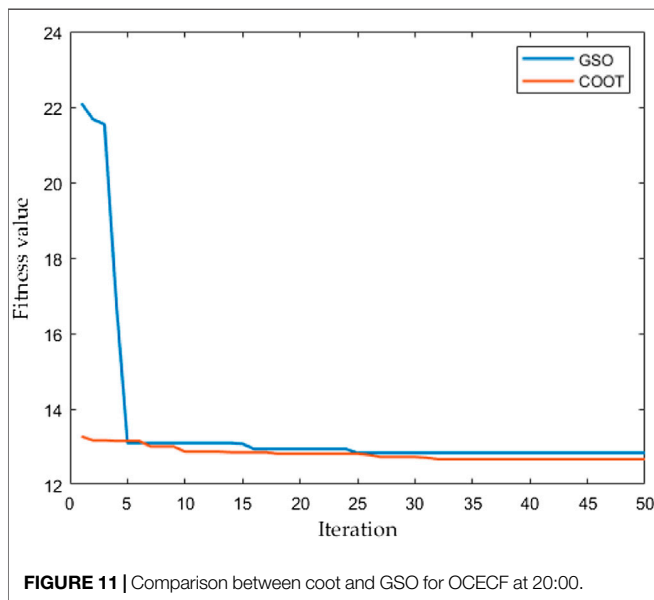


FIGURE 11 | Comparison between coot and GSO for OCECF at 20:00.

solution set, while  $\cos(2R\pi)$  is searched with different radii for a better location within this range around the region of best search. The question that tends to arise is how and when these various motions are shown. To guarantee the randomness of the optimization algorithm, all these movements we consider are random. This means that while the algorithm is being executed, the coots can move at random, in a chaining manner or toward the leader team.

### 3.3 Design of Coot for optimal carbon–energy combined flow

#### 3.3.1 Fitness of coots and leaders

To obtain the desired result, minimizing the objective function (6) is the biggest goal. At the same time, each of the constraints in Eq.

TABLE 3 | Result comparison of online optimization under different algorithms at different times.

Time period	Algorithm	$V_d$ (%)	$C_{loss}$ (ton/h)	$P_{loss}$ (MW)	$f$
0:00	GSO	13.589	0.721	9.065	7.770
	Coot	13.142	0.713	9.043	7.694
5:00	GSO	13.341	0.864	10.131	8.112
	Coot	13.264	0.863	10.129	8.058
10:00	GSO	13.508	0.764	9.591	7.954
	Coot	13.097	0.767	9.603	7.823
15:00	GSO	15.890	1.362	12.394	9.882
	Coot	14.437	1.353	12.361	9.384
20:00	GSO	17.720	2.603	17.926	12.720
	Coot	17.364	2.585	17.857	12.631

(7) needs to be satisfied. Therefore, a penalty function approach is used to design this fitness function as follows:

$$Fit(x_j) = \mu_1 P_{loss}^j + \mu_2 C_{pgc}^j + \mu_3 V_d^j + \eta q^j, j \in J^e \quad (19)$$

in which  $\eta$  denotes the punitive element, and  $q$  shows the amount of constraint breached inequalities.

#### 3.3.2 Parameter setting

For the purpose of performing as desired for OCECF in Coot, several significant parameters, such as  $P, N_L, N_{COOT}$ , and  $MaxIter$ , need to be carefully selected by analysis and calculation. A unified design was employed, and several exercises were conducted to ascertain the parameters, the optimum of which is shown in Table 1.

#### 3.3.3 Execution procedure

Figure 4 outlines Coot’s overall execution procedure for OCECF.

## 4 CASE STUDIES

A common power system (IEEE 57 bus system in Figure 5) is selected as the benchmark system and evaluated by dynamic testing in this paper. For performance comparison, the classical heuristic optimization technique glowworm swarm optimization (GSO) algorithm was introduced in the study to perform experiments in OCECF. The simulations were carried out in Matlab R2019a, operated in a laptop with an Intel(R) Core TM i7 CPU with 3.8 GHz and 16 GB of RAM. According to the systematic analysis and research (Zhang et al., 2017), the shares of liability  $\alpha_p$  for producers and  $\beta_c$  for consumers are each defined as 50% and 100%, respectively, to obtain relatively appropriate results. Overall, setting the same preference for each objective facilitates a better analysis, so it is a reasonable choice for the weighting coefficients ( $\mu_1, \mu_2$ , and  $\mu_3$ ) to be set to 1/3 on average. Assuming that the model OCECF is implemented in a 15-min cycle (Zhang et al., 2015), the mission count for 1 day is 96, and five of these typical nodes are selected for comparative analysis in the article.



**TABLE 4** | Values of the optimal carbon–energy combined flow (OCECF) model variables under two different algorithms in the IEEE 57-bus system.

Type	Variable	0:00		5:00		10:00		15:00		20:00	
		GSO	Coot	GSO	Coot	GSO	Coot	GSO	Coot	GSO	Coot
Reactive power compensation (Mvar)	$Q_{C18}$	2	3	3	3	2	3	3	5	4	4
	$Q_{C25}$	1	1	3	3	2	1	4	5	5	5
	$Q_{C53}$	3	5	4	5	1	5	4	3	4	5
Transformer taps	$k_{4-18}$	0.98	1.02	1.02	1.02	1.02	0.98	1.02	1.02	1.02	1.04
	$k_{21-20}$	1.02	1.02	0.98	1.00	1.00	1.00	0.98	1.00	0.98	0.98
	$k_{34-32}$	0.96	0.96	0.96	0.96	0.96	0.96	0.96	0.96	0.96	0.96
	$k_{39-57}$	0.98	0.96	0.96	0.96	0.96	0.96	0.96	0.96	0.98	0.96
	$k_{7-29}$	1.00	0.98	0.98	0.98	0.98	0.98	0.98	0.98	0.98	0.98
	$k_{9-55}$	0.96	0.98	1.00	0.98	0.98	0.98	0.96	0.98	0.98	0.98

## 4.1 System model

The IEEE 57-bus system includes seven generators, and the carbon intensity  $\delta_w$  for every single power producer is presented in **Table 2**. In addition, a detailed layout of the topology of the IEEE 57-bus system is supplied in **Figure 7**. The main parameters of regulation of the units are given in **Table 1**. Both the stock size of the algorithm and the maximal amount of the iterative strides were given to 50.

## 4.2 Experiments and comparison

To help weigh the choice of algorithms in engineering applications, GSO, an algorithm with fast convergence and high-quality obtained solution sets, is introduced to test and compare the optimized performance online of Coot with the Coot algorithm proposed on the OCECF model. Compared with GSO, it is clearly described that Coot can acquire the most optimal and efficient approach toward the task due to its efficient exploitation. It is evident from the simulation plots that the GSO algorithm tends to fall into local optima, converges more slowly, and obtains worse fitness than Coot. This fully verifies the excellent global searching ability of Coot.

To evaluate the capability at the Coot operator, the online optimizing outputs of five conditions are compared in this example, as shown in **Figures 6–11**, where precision is used to approximate the simulation time for the actual regulated export and the curve of the regulating instructions. It is possible to notice that COOT has a significant empirical advantage compared with GSO. **Table 3** shows the comparison of online optimization results under two different algorithms, while the optimal values of all the controllable variables are provided in **Table 4**. It can be found that COOT can acquire the smaller fitness function than GSO, thus, the voltage deviation, CO<sub>2</sub> exhaust, and electric consumption can be dramatically decreased.

## 5 CONCLUSION

In a nutshell, this study comprises the contribution of the following three aspects.

- 1) From a practical point of view, the constructed OCECF can take the participation of aluminum plants into account; thus, the CO<sub>2</sub> emission about the whole electricity supply system can be significantly reduced, especially on the part of the power grid.
- 2) A fast search algorithm for a solution set obtained by imitating the water movement of birds is applied to the model. Coot algorithm can implement a wide exploration *via* the random movement and a deep exploitation *via* the chain movement with the group leaders. Hence, a high-quality optimal solution can be acquired for OCECF.
- 3) It is confirmed from experiments that the Coot algorithm has more significant advantages in improving the convergence speed by an order of magnitude and guaranteeing the quality of the optimal solution compared with GSO.

## DATA AVAILABILITY STATEMENT

The original contributions presented in the study are included in the article/Supplementary Material. Further inquiries can be directed to the corresponding author.

## AUTHOR CONTRIBUTIONS

Conceptualization, LQ; Methodology, TX; Investigation, SL; Project administration, ZC; Resources, QZ; Formal analysis, JT; Supervision, YL; Writing—original draft, LQ.

## FUNDING

This work is supported by research on carbon emission monitoring modeling method and low-carbon transformation strategy of key industries for carbon peaking and carbon neutrality goals (B704JY210069).

## REFERENCES

- Abbas, G., Gu, J., Farooq, U., Raza, A., Asad, M. U., and El-Hawary, M. E. (2017). Solution of an Economic Dispatch Problem through Particle Swarm Optimization: A Detailed Survey - Part II. *IEEE Access* 5, 24426–24445. doi:10.1109/access.2017.2768522
- Adhvaryu, P. K., Chattopadhyay, P. K., and Bhattacharya, A. (2017). Dynamic Optimal Power Flow of Combined Heat and Power System with Valve-point Effect Using Krill Herd Algorithm. *Energy* 127 (15), 756–767. doi:10.1016/j.energy.2017.03.046
- Carpentier, P., Gohén, G., Culioli, J.-C., and Renaud, A. (1996). Stochastic Optimization of Unit Commitment: A New Decomposition Framework. *IEEE Trans. Power Syst.* 11, 1067–1073. doi:10.1109/59.496196
- Cook, R., Chang, I. T. H., and Falticeanu, C. L. (2007). Aluminium and Aluminium alloy Powders for P/M Applications. *MSF* 534-536, 773–776. doi:10.4028/www.scientific.net/msf.534-536.773
- Gan, W., Ai, X., Fang, J., Yan, M., Yao, W., Zuo, W., et al. (2019). Security Constrained Co-planning of Transmission Expansion and Energy Storage. *Appl. Energy* 239, 383–394. doi:10.1016/j.apenergy.2019.01.192
- Ghorbani, N. (2016). Combined Heat and Power Economic Dispatch Using Exchange Market Algorithm. *Int. J. Electr. Power Energy Syst.* 82, 58–66. doi:10.1016/j.ijepes.2016.03.004
- Kang, C., Zhou, T., Chen, Q., Xu, Q., Xia, Q., and Ji, Z. (2012). Carbon Emission Flow in Networks. *Sci. Rep.* 2, 479–226. doi:10.1038/srep00479
- Lassagne, O., Gosselin, L., Désilets, M., and Iliuta, M. C. (2013). Techno-economic Study of CO<sub>2</sub> Capture for Aluminum Primary Production for Different Electrolytic Cell Ventilation Rates. *Chem. Eng. J.* 230, 338–350. doi:10.1016/j.ccej.2013.06.038
- Li, B., Song, Y., and Hu, Z. (2013). Carbon Flow Tracing Method for Assessment of Demand Side Carbon Emissions Obligation. *IEEE Trans. Sustain. Energy* 4 (4), 1100–1107. doi:10.1109/tste.2013.2268642
- Liu, P., Fu, Y., and Kargarian marvasti, A. (2014). Multi-stage Stochastic Optimal Operation of Energy-Efficient Building with Combined Heat and Power System. *Electr. Power Compon. Syst.* 42, 327–338. doi:10.1080/15325008.2013.862324
- Memarzadeh, G., and Keynia, F. (2021). A New Optimal Energy Storage System Model for Wind Power Producers Based on Long Short Term Memory and Coot Bird Search Algorithm. *Energy Storage* 44, 103401. doi:10.1016/j.est.2021.103401
- Naruei, I., and Keynia, F. (2021). A New Optimization Method Based on Coot Bird Natural Life Model. *Expert Syst. Appl.* 183 (30), 115352. doi:10.1016/j.eswa.2021.115352
- Walther, G. R., Post, E., Convey, P., Menzel, A., Parmesan, C., Beebee, T. J., et al. (2002). Ecological Responses to Recent Climate Change. *Nature* 416, 389–395. doi:10.1038/416389a
- Wei, W., Liu, F., Wang, J., Chen, L., Mei, S., and Yuan, T. (2016). Robust Environmental-Economic Dispatch Incorporating Wind Power Generation and Carbon Capture Plants. *Appl. Energy* 183, 674–684. doi:10.1016/j.apenergy.2016.09.013
- Zhang, X., Chen, Y., Yu, T., Yang, B., Zheng, L., and Huang, L. (2015). Approximate Ideal Multi-Objective Solution  $Q(\lambda)$  Learning for Optimal Carbon-Energy Combined-Flow in Multi-Energy Power Systems. *Energy Convers. Manage.* 106, 543–556. doi:10.1016/j.enconman.2015.09.049
- Zhang, X., Chen, Y., Yu, T., Yang, B., Qu, K., and Mao, S. (2017). Equilibrium-inspired Multiagent Optimizer with Extreme Transfer Learning for Decentralized Optimal Carbon-Energy Combined-Flow of Large-Scale Power Systems. *Appl. Energy* 189 (1), 157–176. doi:10.1016/j.apenergy.2016.12.080
- Zhang, X., Yu, T., Guo, L., Yang, B., and Chen, Y. (2018). Culture Evolution Learning for Optimal Carbon-Energy Combined-Flow. *IEEE Access* 6, 15521–15531. doi:10.1109/access.2018.2815547
- Zhou, B., Fang, J., Ai, X., Yao, W., and Wen, J. (2021). Flexibility-Enhanced Continuous-Time Scheduling of Power System under Wind Uncertainties. *IEEE Trans. Sustain. Energy* 12 (4), 2306–2320. doi:10.1109/tste.2021.3089696
- Zhou, B., Fang, J., Ai, X., Yang, C., Yao, W., and Wen, J. (2021). Dynamic Var Reserve-Constrained Coordinated Scheduling of LCC-HVDC Receiving-End System Considering Contingencies and Wind Uncertainties. *IEEE Trans. Sustain. Energy* 12 (1), 469–481. doi:10.1109/tste.2020.3006984

**Conflict of Interest:** LQ, TX, ZC, QZ, and JT are employed by the Economic Research Institute of State Grid Hebei Electric Power Company.

The remaining authors declare that the research was conducted in the absence of any commercial or financial relationships that could be construed as a potential conflict of interest.

**Publisher's Note:** All claims expressed in this article are solely those of the authors and do not necessarily represent those of their affiliated organizations, or those of the publisher, the editors, and the reviewers. Any product that may be evaluated in this article, or claim that may be made by its manufacturer, is not guaranteed or endorsed by the publisher.

Copyright © 2022 Qin, Xu, Li, Chen, Zhang, Tian and Lin. This is an open-access article distributed under the terms of the Creative Commons Attribution License (CC BY). The use, distribution or reproduction in other forums is permitted, provided the original author(s) and the copyright owner(s) are credited and that the original publication in this journal is cited, in accordance with accepted academic practice. No use, distribution or reproduction is permitted which does not comply with these terms.